Aalto University

OPEN ACCESS

This is an electronic reprint of the original article.
This reprint may differ from the original in pagination and typographic detail.

Zubiaga, A.; Plazaola, F.; Garcia, J.A.; Tuomisto, Filip; Munoz-San Jose, V.; Tena-Zaera, R.

Positron annihilation lifetime spectroscopy of ZnO bulk samples

Published in:
Physical Review B

DOI:
10.1103/PhysRevB.76.085202

Published: 01/08/2007

Document Version
Publisher's PDF, also known as Version of record

Please cite the original version:
Zubiaga, A., Plazaola, F., Garcia, J. A., Tuomisto, F., Munoz-San Jose, V., & Tena-Zaera, R. (2007). Positron annihilation lifetime spectroscopy of ZnO bulk samples. *Physical Review B*, *76*(8), 1-8. [085202]. https://doi.org/10.1103/PhysRevB.76.085202

This material is protected by copyright and other intellectual property rights, and duplication or sale of all or part of any of the repository collections is not permitted, except that material may be duplicated by you for your research use or educational purposes in electronic or print form. You must obtain permission for any other use. Electronic or print copies may not be offered, whether for sale or otherwise to anyone who is not an authorised user.

Positron annihilation lifetime spectroscopy of ZnO bulk samples

A. Zubiaga,* F. Plazaola, and J. A. García
Fisika Aplikatua II Saila, Euskal Herriko Unibertsitatea, Posta Kutxatila 644, 48080 Bilbao, Spain

F. Tuomisto
Laboratory of Physics, Helsinki University of Technology, P.O. Box 1100, 02015 TKK, Espoo, Finland

V. Muñoz-Sanjosé and R. Tena-Zaera†
Departament de Fisica Aplicada i Electromagnetisme, c/ Doctor Moliner 50, E-46100 Burjassot, Valencia, Spain
(Received 10 August 2006; revised manuscript received 20 June 2007; published 2 August 2007; corrected 6 August 2007)

In order to gain a further insight into the knowledge of point defects of ZnO, positron annihilation lifetime spectroscopy was performed on bulk samples annealed under different atmospheres. The samples were characterized at temperatures ranging from 10 to 500 K. Due to difficulties in the conventional fitting of the lifetime spectra caused by the low intensity of the defect signals, we have used an alternative method as a solution to overcome these difficulties and resolve all the lifetime components present in the spectra. Two different vacancy-type defects are identified in the samples: Zn vacancy complexes (V_{Zn}-X) and vacancy clusters consisting of up to five missing Zn-O pairs. In addition to the vacancies, we observe negative-ion-type defects, which are tentatively attributed to intrinsic defects in the Zn sublattice. The effect of the annealing on the observed defects is discussed. The concentrations of the V_{Zn}-X complexes and negative-ion-type defects are in the 0.2–2 ppm range, while the cluster concentrations are 1–2 orders of magnitude lower.

DOI: 10.1103/PhysRevB.76.085202 PACS number(s): 61.72.Ji, 78.70.Bj, 61.82.Fk

I. INTRODUCTION

The fabrication of photonic devices of ultraviolet wavelength range and high frequency electronic devices requires semiconductors with a wide band gap. The physical and chemical properties of ZnO make it a promising candidate for optoelectronic applications in the blue-UV range.[1] ZnO is a semiconducting compound of the II-VI family with a direct wide band gap (3.37 eV at room temperature) and it presents an exciton binding energy of 60 meV.[2] As a consequence, the excitons are not easily thermally dissociated and the near band gap recombination is very efficient even at room temperature. In addition, the electrical and optical properties of ZnO are very resistant to deterioration under irradiation.[3]

Defects and impurities in semiconductors can trap electrons and holes. The electronic and optical properties of the devices are largely affected by the defects and their presence must be controlled. As-grown ZnO samples are *n* type, but if a *p*-*n* junction is to be constructed, ZnO bulk samples of *p*-type conductivity need to be obtained. Great effort is being put into obtaining *p*-type bulk samples. Nitrogen,[4] phosphorus,[5] and arsenic[6] are potential acceptor impurities, but it is difficult to obtain crystals with stable *p* character.[2]

The creation of excess donors is determined by the thermodynamics and the growth process. Many parameters, such as the partial pressure of the components or the growth temperature, control this process. In thermodynamical equilibrium, the concentration of the defects is determined by their formation energy. In subsequent thermal treatments, the autodiffusion of vacancies and interstitials can decrease their concentration. Positron annihilation lifetime spectroscopy (PALS) is a useful tool for studying open volume defects in semiconductors.[7] Positrons get trapped at negative and neutral vacancy defects, and also at hydrogenic states around negatively charged defects with no open volume, such as acceptor-type impurities.

In this work, we study ZnO bulk crystals, grown by vapor transport (VT), annealed under different atmospheres: oxygen vapor overpressure, Zn vapor overpressure, and vacuum. PALS measurements have been performed from 10 to 500 K. The origin of the observed defects and their behavior in the annealed samples are discussed.

II. EXPERIMENT

As said before, ZnO bulk samples were grown by VT under slightly Zn-rich conditions.[8] The samples were annealed at 900 °C for 20 h in atmosphere composed of oxygen (O_2) vapor 2 atm overpressured, in atmosphere composed of Zn vapor 2 atm overpressured, and in vacuum. A couple of identical samples are necessary to measure the positron annihilation lifetime. Then, all the annealed and the as-grown samples were cut from the same ingot for a direct comparison of the differences and their characteristics.

The PALS measurements were performed with a fast-fast spectrometer in collinear geometry[7] in the 10–500 K temperature range. The time resolution of the experimental setup was 270 ps. As positron source, we used ^{22}NaCl deposited on a thin Al foil, sandwiched between two sample pieces. All spectra have $(1.7–2)\times10^6$ counts and the lifetime spectra were analyzed after subtracting the background and the source corrections (215 ps 3%, 400 ps 5.1%, 1500 ps 0.09%) determined with a saturated vapor pressure (SVP)-grown reference ZnO sample.[9] The analyses were performed with two lifetimes convoluted with the Gaussian resolution function of the experimental setup. The average lifetime (τ), which coincides with the center of mass of the spectrum, has the smallest experimental error, so the changes in the average lifetime are the best evidence of changes in the composition of the defects. It can be calculated as the sum of the indi-

 ©2007 The American Physical Society

vidual lifetimes, weighted with the normalized intensity of each component: $\tau = \Sigma_i I_i \tau_i$. The increase of the average lifetime above the positron lifetime in the bulk (τ_b) indicates the presence of vacancy-type defects. The kinetic trapping model[10] is used to fit the experimental positron lifetime data.

III. POSITRON TRAPPING AT DEFECTS

When a positron enters a semiconductor material, it loses its kinetic energy rapidly and reaches thermal equilibrium with the crystal lattice. It diffuses through the material until it annihilates directly from the delocalized state with an electron, or gets trapped at a defect and annihilates from a localized state. Neutral and negatively charged vacancy defects are efficient positron traps due to the missing positive ion core. Also, negatively charged defects with no open volume can trap positrons at low temperatures. The positron lifetime correlates with the open volume at the annihilation site; hence, it is longer at vacancy defects than in the free state in the lattice. In the case of neutral defects, the positron trapping is independent of the temperature, but the trapping coefficient of negatively charged defects[10] varies as $T^{-1/2}$.

The positron trapping rate to a defect (κ_D) is proportional to its concentration (C_D): $\kappa_D = \mu_D C_D$. The trapping coefficient (μ_D) depends on the type of the defect and the surrounding lattice.[11] The trapping and annihilation processes are described by a set of kinetic equations. They relate the rate of change of density of positrons in a determined state to the trapping, detrapping, and annihilation rates at all the states of the positron.[10]

In addition to vacancy defects, positrons can also get trapped at hydrogenlike Rydberg states surrounding negative centers with no open volume (called ionic traps from this point forward), where their binding energy is small (typically $E_b \leqslant 0.1$ eV). Positrons are not well localized at the ionic traps and their wave functions extend to the bulk of the material; hence, the annihilation characteristics are similar to the delocalized state in the lattice and they get detrapped below room temperature.[12] The detrapping process from the ionic traps is thermally activated and the activation energy is equal to the binding energy E_b.[13] The escape rate (δ_{ion}) can be written as

$$\delta_{ion} = \kappa_{ion} \frac{(2\pi m^* k_B T/h^2)}{c_{ion}}^{3/2} e^{(-E_b/k_B T)}, \quad (1)$$

where $m^* \simeq m_0$ is the positron effective mass, k_B the Boltzmann constant, c_{ion} the ion concentration, and h the Planck constant. In principle, positrons can also escape from the Rydberg states around negatively charged vacancies, but we assume that the transition from the Rydberg state to the ground state in the vacancy is fast enough so that this effect can be neglected.[10] An effective trapping rate of the ionic traps can thus be defined as

$$\kappa_{ion}^{eff} = \frac{\kappa_{ion}}{1 + \delta_{ion}/\lambda_{ion}}, \quad (2)$$

where $\lambda_{ion} = \lambda_b = \tau_b^{-1}$ is the annihilation rate of positrons trapped at the Rydberg state, which coincides with the annihilation rate from the delocalized state in the lattice.

We will show in this work that the analyzed ZnO samples contain two different types of vacancy defects (Zn vacancy complex defects, V_{Zn}-X, and vacancy clusters) and ionic traps. In this case, the average lifetime is related to the positron trapping rates and annihilation lifetimes in the four different states as follows:

$$\tau = \tau_b + \frac{\kappa_v(\tau_v - \tau_b) + \kappa_{cl}(\tau_{cl} - \tau_b)}{\frac{1}{\tau_b} + \kappa_{ion}^{eff} + \kappa_v + \kappa_{cl}}. \quad (3)$$

At temperatures high enough, positrons escape efficiently from the ionic traps and the experimental values can be analyzed with the assumption that only vacancy-type defects contribute to the data. In addition, if only one vacancy type contributes to the annihilation spectra, the annihilation parameters can be estimated using the equations of the one-vacancy-type defect trapping model:

$$\kappa_v = \frac{1}{\tau_b} \frac{\tau - \tau_b}{\tau_v - \tau}, \quad (4)$$

$$\tau_1^* = \frac{\tau_b}{1 + \tau_b \kappa_v}, \quad (5)$$

where $\tau_v = \tau_2$, the longer lifetime in the decomposition of the lifetime spectra.

The trapping rate at ionic traps (κ_{ion}) can be calculated at low temperatures, where the escape rate is small enough to be neglected, using the following relation:

$$\kappa_{ion} \simeq \kappa_{ion}^{eff} = \frac{\kappa_v(\tau_v - \tau) + \kappa_{cl}(\tau_{cl} - \tau) + \lambda_b(\tau_b - \tau)}{\tau - \tau_{ion}}. \quad (6)$$

Due to finite time resolution, annihilations at source material, and background noise, usually only one or two lifetime components are resolved in the experimental spectrum. The longest lifetime of the decomposition corresponds to the lifetime of positrons trapped at vacancy-type defects. If the lifetime difference of two annihilation states is not large enough ($\Delta\tau \sim 20\% - 30\%$), they will appear mixed in a single lifetime component in the fitting. The shortest lifetime is a superposition of the positron lifetime in the delocalized state, that at the ionic traps, and that at the vacancy-type defects.

IV. RESULTS

Figure 1 shows the average lifetime measured at temperatures ranging from 10 to 500 K. A SVP-grown reference sample has also been measured at 300 K. The vacancy concentration in this sample is very low, and at room temperature only annihilations in the bulk are observed, giving an average positron lifetime of 171 ps, in good agreement with the lifetime measured in this sample at room temperature in Ref. 9. The average positron lifetime in all the VT-grown samples is above the bulk lifetime. This is a clear indication that positrons are trapped at vacancy defects. The average positron lifetime in the Zn annealed sample is 5–6 ps lower

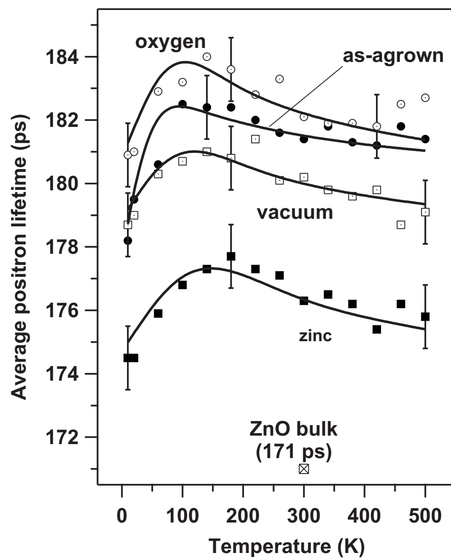

FIG. 1. The average positron lifetime in the ZnO samples annealed under different conditions, measured in the temperature range from 10 to 500 K. Also, the bulk lifetime measured in the SVP-grown reference sample is shown. The solid lines show the average positron lifetime fitted with the kinetic trapping model.

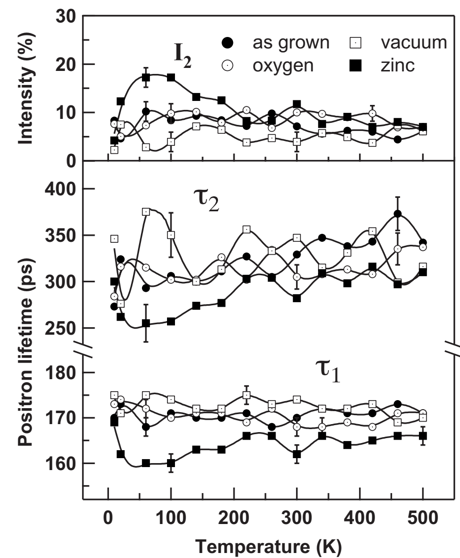

FIG. 2. Decomposition of the lifetime of all measured samples in the full temperature range.

than that in the as-grown sample in the whole measurement temperature range, and the Zn annealed sample has the lowest lifetime values among the measured samples. The average lifetime in the oxygen annealed sample is 3 ps higher than that in the as-grown sample at 10 K, but it is only 1 ps higher at 500 K. On the other hand, the average lifetime in the vacuum annealed sample is similar to that measured in the as-grown sample at 10 K and 2 ps lower at 500 K.

The decrease of the average positron lifetime with increasing temperature (Fig. 1) above 200 K is an indication of the vacancy defects being in the negative charge state. This behavior is due to the $T^{-1/2}$ dependence of the positron trapping coefficient to negative centers. Below 200 K, the average positron lifetime decreases strongly with decreasing temperature. This is explained by the enhancement of positron trapping at negative-ion-type defects (with no open volume), from which the positron escapes at higher temperatures.

Figure 2 shows the results obtained by fitting the spectra with two lifetimes as free parameters. If we focus on temperatures above 200 K, we can observe that the values of the higher lifetime component (τ_2) and its intensity (I_2) in all the measured samples are almost similar within the experimental error. Also, the lower lifetime components (τ_1) in the as-grown, the oxygen annealed, and the vacuum annealed samples have similar values. However, τ_1 in the sample annealed under Zn atmosphere is shorter over the whole temperature range. The differences in the lifetime components between the samples at temperatures below 200 K are larger.

The value of τ_2 is clearly larger than the values reported for the Zn vacancy. It ranges between 300 and 350 ps for temperatures higher than 200 K and τ_2/τ_b is around 1.7–2.0. This value is higher than the typical value for monovacancies in semiconductors.[10,14] Hence, defects with larger open volume, i.e., vacancy clusters, contribute to τ_2.

V. DISCUSSION

A. Positron lifetime in the ZnO lattice

Results of positron measurements in bulk ZnO crystals grown by EaglePicher (EP), the material used as reference in this work, have been reported earlier by three different groups.[9,15,16] The conclusions in these works coincide: the vacancy defect concentration in this material is below the detection limit of positron annihilation spectroscopy and only one lifetime component can be fitted to the spectrum at room temperature, thus giving directly the bulk lifetime. Hence, the EP ZnO samples are ideal for use as a reference. The bulk lifetime values reported by Brunner *et al.*[15] and Uedono *et al.*[16] (161 and 158 ps, respectively) are slightly lower than that reported by Tuomisto *et al.*[9] (171 ps). However, slight differences in the positron lifetime spectrometers, such as scintillators, geometry, and electronic settings, influence the absolute values of the positron lifetimes. In addition, the source corrections used are reported only in Refs. 9 and 17, which makes the direct comparison of the absolute values even less meaningful. Very recently,[18] a bulk lifetime as low as 151 ps was also reported (in melt-grown material) from a lifetime spectrum with 1×10^6 counts measured at room temperature in a setup with a resolution of 250 ps, but this value was estimated from a lifetime spectrum dominated by a vacancy-related lifetime of 257 ps (intensity of 60%), and as such it is difficult to compare in a straightforward way with directly measured values. The source corrections used were not given in this report either.

The above discussion demonstrates the importance of having high-quality (low vacancy defect concentration) material, such as the EP bulk crystal, as a reference sample for positron measurements. In addition to as-grown samples, electron-irradiated ZnO has also been studied by Brunner *et al.*[15] They report a Zn-vacancy-related lifetime of 210 ± 10 ps, somewhat lower than the value obtained by Tuomisto *et al.*[9] (230 ± 10 ps). The important value in the

identification of different vacancy defects is the ratio τ_D/τ_B of the defect-related and bulk lifetimes. As the bulk lifetime measured with the setup of Brunner *et al.*[15] is lower, the agreement between the Zn vacancy values obtained by the two groups is very good (the ratios are $\tau_D/\tau_B=1.30\pm0.05$ and $\tau_D/\tau_B=1.35\pm0.05$, respectively). In addition to the irradiated ZnO, a value of 230 ± 10 ps has been obtained for Zn vacancies in as-grown material as well,[19] measured with the same setup as in this work.

As the EP ZnO reference sample, on which all previous works by different groups agree to have a vacancy defect concentration below the PAS detection limit, gives in the setup used in the present measurements a single lifetime of 171 ps at room temperature, this lifetime is used as the bulk lifetime in ZnO in this work. Consequently, 230 ps is used as the Zn vacancy specific lifetime. Finally, it is worth noticing that in order to test the quality of the measured lifetimes, defect-free Si and GaAs standard references were measured with the same setup to give bulk lifetimes of 220 ± 1 and 231 ± 1 ps, respectively. These values are in excellent agreement with the values widely reported in the literature: $\tau_B=219-222$ ps for bulk Si (see, e.g., Ref. 20 and references therein) and $\tau_B=228-232$ ps for bulk GaAs (see, e.g., Ref. 21 and references therein).

B. Fitting procedure

Fitting the spectra using two lifetimes as free parameters shows that τ_1 in the Zn annealed sample is systematically lower than in the other samples (Fig. 2). This feature correlates with the lower value of the average lifetime in this sample. The other parameters (τ_2 and I_2) do not show any clear difference between the Zn vapor annealed sample and the other samples. Moreover, τ_1 is a statistically strong parameter due to the large value of I_1 ($\sim$90%) in all the measured samples and temperatures.

We tested the one-vacancy trapping model by comparing the fitted τ_1 of all the samples in the decomposition analysis of the spectra with two lifetimes as free parameters, with τ_1^* obtained from the model. Here, we used the fitted τ_2 as the vacancy lifetime at each temperature. The agreement between the fitted τ_1 and τ_1^* obtained from the one-vacancy model is good only in the Zn vapor annealed sample (Fig. 3). In the other samples, τ_1^* is systematically below the fitted value. This result can be well understood if the Zn annealed sample contains only one type of vacancy defects and the other samples contain at least two different types of vacancy-related defects. It must be noted that τ_1 is below τ_b in the Zn annealed sample, as expected when only one kind of vacancy is present. The same conclusion is reached by fixing the higher lifetime component to 340 ps, the average value of the fitted τ_2.

Fitting the experimental spectra with three lifetime components (either as free or fixed) does not work due to the low intensity (total about 10%) of the longer components. The main problems in the analysis are the rather low intensity of the higher lifetime component and the fact that different vacancy-type defects are present in the material with lifetimes in the range 170–350 ps. Hence, focusing on the effects in τ_1 (with intensity $\sim$90%) is reasonable.

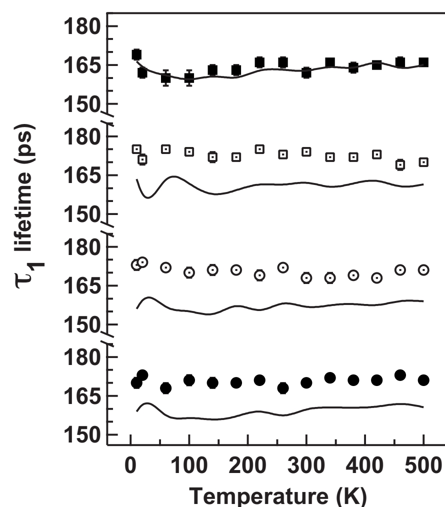

FIG. 3. The lower lifetime component τ_1 of the figure obtained from a fit with two lifetime components as free parameters (markers) and the estimated value from the one-vacancy-type defect model τ_1^* (solid lines), using Eq. (5).

The above analysis indicates that three different lifetimes contribute to the annihilation spectra: the bulk lifetime of $\tau_b\simeq170$ ps, the lifetime specific to vacancy clusters of $\geqslant300$ ps, and a third lifetime somewhere between these two. This component is mixed to both fitted lifetimes when two lifetime components are used as free parameters.

In recent studies on bulk ZnO crystals, negatively charged Zn vacancies[9] and Zn-vacancy-related complexes in the neutral charge state[19] have been observed and their lifetime was 230 ps. The improvement of the results using the one-vacancy model for the fitting of the lifetime corresponding to the Zn vapor annealed samples suggests that the presence of Zn vacancies or related complexes with a lifetime of 230 ps can be responsible for the problems in fitting the experimental lifetime with two free parameters.

Having in mind the similarities between the growth processes in this work and in Ref. 19, we can assume that Zn vacancies or related complexes in a neutral charge state can be present in our samples as well. Taking into account that theoretical calculations predict lower formation energy for Zn vacancies double negative charged than for neutral ones,[22] the neutral state charge felt by positrons points toward the presence of V_{Zn}-X neutral complexes. Thus, Zn vacancies could be complexed with donor-type defects (X) with no open volume or oxygen vacancies with low open volume.

As said before, the fitting with three components is not possible due to the low intensity of the higher components. Hence, assuming their neutrality, we proceed by subtracting a constant contribution as a function of temperature of the Zn vacancies or related complexes (lifetime $\tau_v=230$ ps) from the spectra before fitting two lifetime components. Then, we optimize the subtracted intensity by comparing the fitted τ_1 with τ_1^*, which should coincide when only one-vacancy defect contributes to the spectrum. The intensity of the subtracted component is proportional to the fraction of positrons (η_v) trapped at the defect responsible for this component:

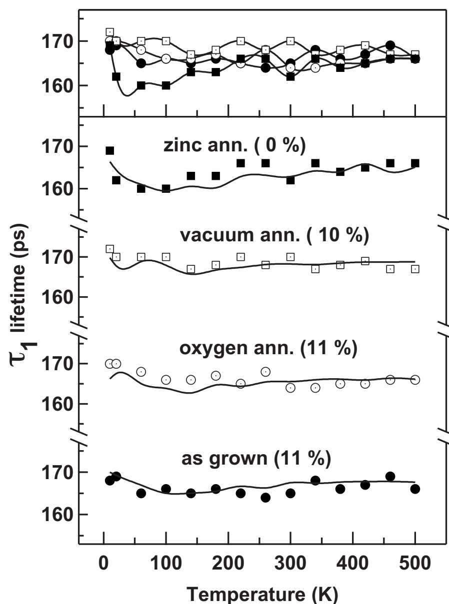

FIG. 4. A constant fraction of the 230 ps component of the spectra has been subtracted from the spectra before obtaining lifetime components. Fit of τ_1 using the one-vacancy-type defect model is shown. Value between parentheses is the subtracted fraction yielding the best result. In the upper graph, overlap of τ_1 of all samples can be observed, specially at temperatures above 200 K.

$$I_v = \frac{\eta_v}{\tau_v} e^{(-t/\tau_v)}. \tag{7}$$

The obtained best values of τ_1 are shown in Fig. 4 in the full range of temperatures. The subtracted fraction of 230 ps lifetime is also shown. The analysis can only be done at temperatures above 200 K, where the effects of the ionic traps can be neglected. In the Zn vapor annealed sample, the best fit is obtained if the 230 ps component is not subtracted at all. If the subtracted intensity is varied around the optimal value, the comparison to the one-vacancy trapping model is weakened. This analysis supports the existence of two types of vacancy defects in the samples.

Hence, we conclude that the lifetime spectra have contributions from two types of vacancy defects at high temperatures: one of around 230 ps, associated with Zn vacancies or related complexes, that cannot be resolved in ordinary decompositions, and another of around 300–350 ps, associated with vacancy clusters. The Zn vapor annealed sample at temperatures above 200 K has zero intensity of the 230 ps lifetime and positrons are trapped at one type of vacancy defects in this sample. The other samples are optimally fitted when the subtracted fractions are 9% (vacuum annealed sample) and 10% (as-grown and oxygen annealed samples). The procedure to arrive at the above results is as follows.

(1) The spectra are fitted using two lifetimes as free parameters, obtaining results with lower statistical noise than with three lifetimes, and a complete separation of the vacancy-type defect contributions has been obtained.

(2) The analysis is tested using the one defect trapping model.

(3) The criterion $\tau_1 = \tau_1^*$ for the subtraction of the right intensity value is used.

TABLE I. The first column shows the trapping fractions of the 230 ps lifetime defect subtracted during the fitting of the spectra. The subsequent columns show the trapping fractions, trapping rates at 300 K, and concentrations of Zn vacancies in the samples obtained by fitting the average lifetime. The concentration of the Zn vacancies in the Zn annealed sample is below the detection limit.

	Subtracted (%)	Fitted (%)	κ_v^0 (ns^{-1})	C_v (ppm)
As grown	11	14	0.9(1)	0.3
Oxygen	11	12	0.8(1)	0.3
Vacuum	10	9	0.6(1)	0.2
Zn				$\leqslant$0.03

While making this analysis, only the 200–500 K temperature range has been considered, because at low temperatures positrons also annihilate at ionic traps. The presence of only one type of defect in the spectra besides the 230 ps component is necessary to apply this analysis. The subtraction of a constant intensity independent of temperature gives a very good agreement with the one-vacancy model, suggesting that the Zn vacancies belong to V_{Zn}-X neutral complexes in VT-grown ZnO.

C. Concentrations of the defects

The above discussion shows that above 200 K, positrons annihilate mainly at two positron traps: the Zn vacancy or related complexes (τ_V=230 ps) and a vacancy cluster with a longer lifetime. The lifetime of positrons trapped at vacancy clusters can be estimated as an average of the values of τ_2 obtained after the subtraction of the 230 ps component, $\tau_{cl} = \tau_2 = 340 \pm 40$ ps. In this temperature range, the effects of ionic traps and the variations due to the possible temperature dependence of the trapping rates are very small.

Further support of the fact that the Zn vacancies belong to V_{Zn}-X neutral complexes is the temperature variation of the average positron lifetime above 200 K in the Zn vapor annealed sample, where no Zn vacancies are present. Hence, the vacancy clusters are in the negative charge state. As the fitting of three lifetimes to the spectra is uncertain, we fit the average lifetime vs temperature data in the way described in the following [using Eq. (3)].

First, the high temperature range (200–500 K) is fitted considering two vacancy lifetimes: one of 230 ps and another of 340 ps, the effect of ionic traps being negligible at these temperatures. Next, the entire temperature range will be fitted using the trapping rates at vacancies obtained in the first step as fixed parameters to obtain the trapping rate, the concentration, and the binding energy of the ionic traps.

The values obtained after fitting the high temperature range are summarized in Tables I and II. V_{Zn}-X neutral complexes were fitted with a constant trapping rate ($\kappa_v = \kappa_v^0$) and the vacancy clusters with $\kappa_{cl} = \kappa_{cl}^0 (T/300\text{ K})^{-0.5}$, as corresponds to negatively charged defects. The concentrations of V_{Zn}-X-complex-type defects were calculated using the typical trapping coefficient for neutral vacancies in

TABLE II. Trapping rates at 300 K and the concentrations of vacancy clusters obtained by fitting τ in Eq. (3), with trapping rates as fitting parameters.

	κ_{cl}^0 (ns^{-1})	C_{cl} (ppm)
As grown	0.10(2)	0.010(2)
Oxygen	0.18(3)	0.018(3)
Vacuum	0.14(4)	0.014(4)
Zn	0.17(2)	0.017(2)

semiconductors,[7] $\mu_v^0 = 2\times10^{15}$ s^{-1}. The trapping coefficient of vacancy clusters can be estimated[23] as $\mu_{cl}^0 = N\mu_v^0$, where $N\simeq5$ is the number of Zn-O pairs in the cluster, giving $\mu_{cl}^0 = 1\times10^{16}$ s^{-1}.

The concentration of V_{Zn}-X neutral complexes in Zn annealed sample is below the detection limit of about 0.03 ppm. In the oxygen and vacuum annealed samples, the V_{Zn}-X complexes are practically unaffected by the annealings, in good agreement with recent work on chemical vapor transport (CVT) ZnO oxygen annealed samples.[19] In contrast, the concentration of vacancy clusters is higher in all the annealed samples than in the as-grown sample. It is worth noticing that the trapping coefficient at 300 K is higher for vacancy clusters than for V_{Zn}-X complexes. In addition, the clusters are in the negative charge state; as a consequence, the detection limit is lower than that of the V_{Zn}-X complexes, about 0.002 ppm.

Assuming that the vacancy clusters are negatively charged and the V_{Zn}-X complexes are neutral yields the best fit of the average lifetime in the 200–500 K temperature range. In addition, we want to point out that the values of the trapping fractions of the 230 ps Zn vacancy component obtained by subtracting the component when fitting the lifetime spectra are consistent with the results obtained by fitting the average lifetime vs temperature data. In addition, the low concentration (below detection limit) of V_{Zn}-X complexes in the Zn vapor annealed sample is observed with both fitting methods.

The average positron lifetime in all the samples decreases with decreasing temperature below 200 K. This indicates that positrons are efficiently trapped at ionic traps at low temperatures. The estimated values of κ_{ion} [Eq. (6)] are shown in Fig. 5 for temperatures lower than 200 K. The trapping rates follow a power law behavior at temperatures below 60–70 K. At higher temperatures, they decrease rapidly because the detrapping from the defects becomes important. It is remarkable that a similar temperature dependence is obtained in all samples, as it would be the case if the same type of defects was present. The power law coefficient takes values between −0.7 and −0.8 (see Table III), in rather good agreement with both the theoretical value of −0.5 (Ref. 13) and experimental values ranging from −0.3 to −0.7 obtained in GaN and ZnO.[24]

The trapping rates and concentrations of the ionic traps are presented in Table III. It is clearly seen that in all the samples, the majority of positrons annihilate as trapped at ionic traps at low temperatures: for example, in the as-grown sample $\kappa_v = 0.9(1)$ ns^{-1}, $\kappa_{cl} = 0.6(1)$ ns^{-1}, and $\kappa_{ion} = 14(4)$ ns^{-1}. The values of κ_{ion} at 10 K (see Table III) are used in the fit of the annihilation parameters of the ionic traps. The trapping rates of the vacancy-type defects are also introduced as fixed parameters. The average lifetime has been fitted in the entire temperature range using Eq. (3). The fitted parameters are the binding energy of positrons at ionic traps (E_b) and the concentration of ions (C_{ion}). The fitted curves are shown in Fig. 1 and the results are presented in Table III. The binding energy at the traps is 30±10 meV, a reasonable value if we consider that nearly all positrons are detrapped at 200 K.

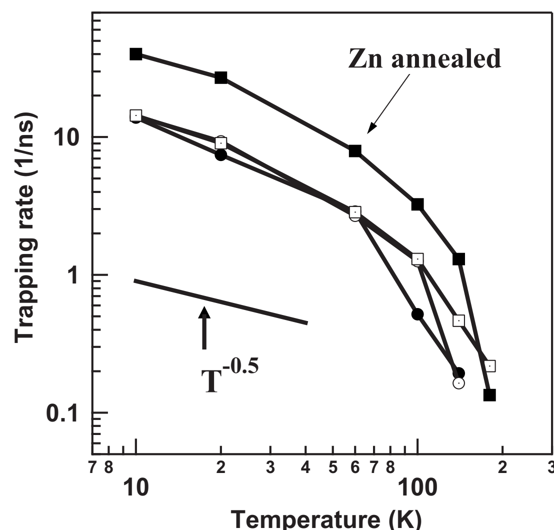

FIG. 5. Logarithmic representation of the estimated κ_{ion} for temperatures below 200 K. The power law behavior is followed up to 60–70 K, where detrapping is negligible. The line representing the theoretical $T^{-0.5}$ power law behavior of negatively charged defects is also shown.

It is worth noticing that the concentration of ionic traps is the highest in the Zn annealed sample (2 ppm obtained from the fit). The concentrations of ionic traps in the other samples are lower and similar (0.4–0.7 ppm). The trapping coefficients of the ionic traps ($\mu_{ion} = \kappa_{ion}/C_{ion}$) get values in the range of $(2-3.5)\times10^{16}$ s^{-1} at 10 K. These values are of the same order of magnitude as the trapping coefficients obtained in GaN.[14]

TABLE III. The estimates for the binding energy of positrons to the ionic trap (E_b), the power law coefficients of the trapping rate (n in T^{-n}), and the concentrations of the ionic traps (C_{ion}) obtained by fitting the average lifetime. The trapping rate to the ionic traps (κ_{ion}) and the estimated trapping coefficients at 10 K (μ_{ion}) are also shown.

	E_b (meV)	n	C_{ion} (ppm)	κ_{ion} (ns^{-1})	μ_{ion} ($\times10^{16}$ s^{-1})
As grown	30(10)	−0.8(1)	0.4(2)	14(4)	3.5
Oxygen	30(10)	−0.7(1)	0.7(3)	14(4)	2.0
Vacuum	30(10)	−0.8(1)	0.6(3)	14(5)	2.3
Zn	30(10)	−0.7(1)	2.0(6)	40(15)	2.0

D. Origin of the defects

Zn vacancies created by irradiation with electrons are recovered at temperatures lower than 600 K.[17] So, the fact that the neutral Zn-vacancy-related defects (τ_V=230 ps) in VT-grown bulk ZnO samples survive the 900 °C annealing in vacuum and oxygen atmospheres is an indication that the Zn vacancies are not isolated, but belong to a V_{Zn}-X defect complex.

The lowest formation energy for the Zn vacancy is for its double negative charge state in *n*-type material.[22] However, the positrons are sensitive to the total charge of the complex, which in this case is neutral. Hence, the Zn vacancies observed in VT-grown are complexed with donor-type defects with no open volume, which can be either impurities or intrinsic defects. Similar neutral in-grown Zn-vacancy-related complexes have also been observed in CVT-grown ZnO.[19] On the other hand, these centers behave in a different way when annealing in Zn atmosphere. Indeed, its concentration decreases below the detection limit of the positron annihilation spectroscopy. So, it indicates that the recovery is not caused by the dissociation and migration of Zn vacancies and it is due to the Zn vapor atmosphere at which it has been annealed. Moreover, Zn interstitials are very mobile at the annealing temperature.[25] Therefore, Zn diffusion into the center must be the cause of the recovery.

The temperature behavior of the longest lifetime component indicates that the vacancy clusters are in the negative charge state. Based on the magnitude of the longest lifetime component (τ_{cl}=340±40 ps), we can estimate the size of the vacancy clusters. This lifetime can be compared to those reported in SiC,[26] where the Si vacancy to SiC bulk lifetime ratio is close to the Zn vacancy to ZnO bulk lifetime ratio. We estimate that the clusters consist of at most five missing Zn-O pairs, as there is no reason to assume that these clusters would be Zn rich or O rich. The concentration of the vacancy clusters increases slightly in all the annealings, suggesting that new clusters are formed during the annealing by the thermal creation and migration of vacancies. The mean size of the clusters does not increase appreciably. It must be pointed out that the vacancy cluster concentration is not increasing at the expense of the Zn-vacancy-related complexes, because they are unaffected by the annealing in vacuum or oxygen atmosphere.

The ionic traps are the most abundant defects observed in our positron experiments. Their presence in as-grown samples has been typically interpreted as them being related to impurities, as the intrinsic defects tend to be mobile at rather low temperatures. However their concentration increases with the annealing in Zn vapor. Hence, we suggest that these negative centers (with no open volume) are related to intrinsic defects in the Zn sublattice.

VI. CONCLUSIONS

We have applied positron annihilation spectroscopy to study the behavior of point defects in the annealing under different conditions of bulk ZnO crystals grown by VT. The positron annihilation lifetime spectra present more than one type of vacancy-type defect and ionic traps. The existence of two types of vacancy-type defect trapping positrons has been unambiguously stated subtracting one lifetime component as a source component before the lifetime analysis. The subtracted intensity has been determined using the one defect trapping model.

The vacancy-type defects are identified as neutral defect complexes involving the Zn vacancy and negatively charged vacancy clusters consisting of at most five missing Zn-O pairs. The concentrations of the Zn vacancies are in the 0.2–0.3 ppm range, while the concentrations of the vacancy clusters are estimated 1–2 orders of magnitude lower. The ionic traps are the most abundant defects observed in our experiments, with concentrations in the 0.5–2 ppm range. The concentration of the Zn-vacancy-related complexes is significantly reduced after annealing in Zn atmosphere. The concentration of the vacancy clusters increases slightly in the annealings, possibly due to the formation and subsequent migration of vacancies on both sublattices. The concentration of the ionic traps increases after annealing in Zn atmosphere, which suggests that they are related to intrinsic defects in the Zn sublattice.

ACKNOWLEDGMENTS

We are thankful for the fruitful discussions with the late K. Saarinen. The work has been undertaken under Projects Nos. MAT2003-406841, MAT2004-06841, MEC872/2006, GV ACOMP06/037, and UPV/EHU-GIU06/59 and with the financial support of the Basque Government under the Researchers Formation Program.

*asier.zubiaga@ehu.es

†Present address: LCMTR, Institut des Sciences Chimiques Seine Amont, CNRS, 2/8 rue Henri Dunant, 94320 Thiais, France.

[1] U. Özgur, Y. Alivov, C. Liu, A. Teke, M. Reshchikov, S. Dogan, V. Avrutin, S. J. Cho, and H. Morko, J. Appl. Phys. **98**, 041301 (2005).

[2] D. C. Look, B. Caflin, Y. I. Alivov, and S. J. Park, Phys. Status Solidi A **201**, 2203 (2004).

[3] D. C. Look, Mater. Sci. Eng., B **80**, 383 (2001).

[4] K. Minegishi, Y. Koiwai, Y. Kikuchi, K. Yano, M. Kasuga, and A. Shimizu, Jpn. J. Appl. Phys., Part 2 **36**, L1453 (1997).

[5] K.-K. Kim, H.-S. Kim, D.-K. Hwang, J.-H. Lim, and S.-J. Park, Appl. Phys. Lett. **83**, 63 (2003).

[6] Y. R. Ryu, S. Zhu, D. C. Look, J. M. Wrobel, H. M. Jeong, and H. W. White, J. Cryst. Growth **216**, 330 (2000).

[7] K. Saarinen, P. Hautojärvi, and C. Corbel, *Semiconductors and Semimetals* (Academic, New York, 1998), p. 209.

[8] R. Tena-Zaera, C. Martinez-Tomas, C. J. Gomez-Garcia, and V. Munoz-Sanjose, Cryst. Res. Technol. **41**, 742 (2006).

[9] F. Tuomisto, V. Ranki, K. Saarinen, and D. C. Look, Phys. Rev.

Lett. **91**, 205502 (2003).
[10] P. Hautojärvi, *Positrons in Solids*, Topics in Current Physics Vol. 12 (Springer, Heidelberg, 1979).
[11] M. J. Puska and R. M. Nieminen, Rev. Mod. Phys. **66**, 841 (1994).
[12] F. Plazaola, K. Saarinen, L. Dobrzynski, H. Reniewicz, F. Firszt, J. Szatkowski, H. Meczynska, S. Legowski, and S. Chabik, J. Appl. Phys. **88**, 1325 (2000).
[13] M. J. Puska, C. Corbel, and R. M. Nieminen, Phys. Rev. B **41**, 9980 (1990).
[14] K. Saarinen, *III-V Nitride Semiconductors: Electrical, Structura and Defect Properties* (Elsevier, Amsterdam, 2000), p. 109.
[15] S. Brunner, W. Puff, A. G. Balogh, and P. Mascher, Mater. Sci. Forum **363-365**, 141 (2001).
[16] A. Uedono, T. Koida, A. Tsukazaki, M. Kawasaki, Z. Q. Chen, S. Chichibu, and H. Koinuma, J. Appl. Phys. **93**, 2481 (2003).
[17] F. Tuomisto, K. Saarinen, D. C. Look, and G. C. Farlow, Phys. Rev. B **72**, 085206 (2005).
[18] G. Brauer, W. Anwand, W. Skorupa, J. Kuriplach, O. Melikhova, C. Moisson, H. von Wenckstern, H. Schmidt, M. Lorenz, and M. Grundmann, Phys. Rev. B **74**, 045208 (2006).
[19] F. Tuomisto, A. Mycielski, and K. Grasza, Superlattices Microstruct. (to be published).
[20] S. Dannefaer, Phys. Status Solidi A **102**, 481 (1987); J. Mäkinen, C. Corbel, P. Hautojärvi, P. Moser, and F. Pierre, Phys. Rev. B **39**, 10162 (1989); K. Saarinen, J. Nissilä, H. Kauppinen, M. Hakala, M. J. Puska, P. Hautojärvi, and C. Corbel, Phys. Rev. Lett. **82**, 1883 (1999).
[21] S. Kuisma, K. Saarinen, P. Hautojärvi, C. Corbel, and C. LeBerre, Phys. Rev. B **53**, 9814 (1996); J. Gebauer, M. Lausmann, F. Redmann, R. Krause-Rehberg, H. S. Leipner, E. R. Weber, and P. Ebert, *ibid.* **67**, 235207 (2003).
[22] A. F. Kohan, G. Ceder, D. Morgan, and Chris G. Van de Walle, Phys. Rev. B **61**, 15019 (2000).
[23] R. M. Nieminen and J. Laakkonen, Appl. Phys. **20**, 181 (1979).
[24] K. Saarinen, S. Hautakangas, and F. Tuomisto Phys. Scr. **T126**, 105 (2006).
[25] Y. V. Gorelkinskii and G. D. Watkins, Phys. Rev. B **69**, 115212 (2004).
[26] G. Brauer, W. Anwand, P. G. Coleman, A. P. Knights, F. Plazaola, Y. Pacaud, W. Skorupa, J. Störmer, and P. Willutzki, Phys. Rev. B **54**, 3084 (1996); G. Brauer, W. Anwand, P. G. Coleman, J. Störmer, F. Plazaola, J. M. Campillo, Y. Pacaud, and W. Skorupa, J. Phys.: Condens. Matter **10**, 1147 (1998); R. Aavikko, K. Saarinen, F. Tuomisto, B. Magnusson, N. T. Son, and E. Janz'en Phys. Rev. B **75**, 085208 (2007).